Bone histology of Iberosuchus macrodon (Sebecosuchia, Crocodylomorpha)

Jorge Cubo, Meike Köhler, Vivian de Buffrénil

Bone histology of *Iberosuchus macrodon* (Sebecosuchia, Crocodylomorpha).

By

Jorge Cubo[1*], Meike Köhler[2, 3], Vivian de Buffrénil[4]

[1] Sorbonne-Universités, UPMC-Univ. Paris 06, CNRS, Institut des Sciences de la Terre de Paris (ISTeP), 4 place Jussieu, BC 19, 75005 Paris, France

[2]ICREA, Pg. Lluís Companys 23, 08010 Barcelona, Spain.

[3] Institut Institut Català de Paleontologia Miquel Crusafont, Universitat Autònoma de Barcelona, Carrer de les Columnes s/n, 08193 Cerdanyola del Vallés, Spain

[4] Museum National d'Histoire Naturelle, Centre de Recherche sur la Paléobiodiversité et les Paléoenvironnements (CR2P), 75005 Paris, France

* Corresponding author : jorge.cubo_garcia@upmc.fr

RH – Bone histology of *Iberosuchus*

17 **ABSTRACT**

18 *Iberosuchus macrodon* is a Cenozoic crocodyliform interpreted as a terrestrial, cursorial form. In
19 order to assess if this adaptation was accompanied by a high growth rate and an elevated resting
20 metabolic rate (two features commonly attributed to several terrestrial Triassic Crocodylomorpha
21 based on histology) we studied bone histology in the femora of two specimens attributed to *I.*
22 *macrodon*. Beyond this question is the broader problem of the possible survival to the Cretaceous-
23 Paleogene extinction event of tachymetabolic sauropsids other than birds. At mid-diaphysis, bone
24 cortices in *Iberosuchus* are made of a parallel-fibered tissue that turns locally to true lamellar bone.
25 Cortical vascularization consists of simple longitudinal canals forming a network of medium density.
26 The spacing pattern of conspicuous lines of arrested growth suggests asymptotic growth for
27 *Iberosuchus*. This general histological structure prevails also in the metaphyseal region of the bones. It
28 is basically similar to that encountered in certain large lizards adapted to active predation, the
29 Varanidae and the Teidae. In one of the two *Iberosuchus* femora, however, an intra-cortical meniscus
30 made of a tissue displaying a global radial architecture, occurs in the region of the fourth trochanter.
31 Histologically, the latter can be interpreted either as compacted spongiosa, or as a fibro-lamellar
32 complex with a gross radial orientation, a tissue corresponding to fast periosteal apposition. These
33 observations suggest that, *Iberosuchus* basically had a slow, cyclical growth indicative of an ecto-
34 poikilothermic, lizard-like, resting metabolic rate. However it might also have retained a limited
35 capacity for fast periosteal accretion in relation to local morphogenetic requirements as, for instance,
36 the development of crests or trochanters.

37 Key-words: Crocodylomorphs, Cretaceous-Paleogene extinction event, terrestriality, bone
38 structure, growth, metabolism.

39

INTRODUCTION

The presence of a four-chambered heart in crocodiles and birds (Seymour *et al*. 2004, Summers 2005) and unidirectional air flow through the lungs (Farmer & Sanders 2010) suggests that the last common ancestor of archosaurs was endothermic, and that this character state was inherited by Ornithodira (pterosaurs and dinosaurs including birds) and Pseudosuchia (taxa more closely related to crocodiles than to birds), but was lost somewhere during the evolution of the latter (Seymour *et al*. 2004). Indirect evidence for this hypothesis has been gained from inferences of bone growth rates of extinct archosaurs (Ricqlès *et al*. 2008; Cubo *et al*. 2012; Legendre *et al*. 2013), assuming a direct relationship between bone growth rates and resting metabolic rates (Montes *et al*. 2007). Recently, resting metabolic rates of extinct archosaurs and non-archosaurian Archosauromorpha were inferred using bone paleohistology (Legendre *et al.* 2016), providing more direct support for that hypothesis.

Interestingly, within Pseudosuchia, aquatic (Dyrosauridae), semiaquatic (Eusuchia) and terrestrial (Sebecidae and other Sebecosuchia such as *Iberosuchus*) forms survived the Cretaceous-Paleogene extinction event (Macleod *et al.* 1997). According to the null hypothesis, *Iberosuchus* retained resting metabolic rates similar to those of Triassic terrestrial Pseudosuchia with an upright stance, such as *Terrestrisuchus* (Ricqlès *et al.* 2003). Two alternative hypotheses will be tested: (1) The inferred cursorial locomotion (Riff & Kellner 2011) of *Iberosuchus* suggests that it might have acquired even higher resting metabolic rates than its Triassic terrestrial relatives. (2) The Cretaceous-Paleogene extinction event filtered the diversity of Pseudosuchia, so that only taxa showing low resting metabolic rates survived. Bone histology has been acknowledged for several decades as one of the major clues for assessing the gross physiological adaptations of extinct taxa (Ricqlès 1974, 1978); unfortunately, there is no description of the histological features of long bones in notosuchians up to now (only osteoderms in some taxa were studied; cf. Buffrénil *et al*. 2015). In order to settle the question, we analyzed the bone histology of *Iberosuchus,* and tentatively interpreted it in terms of growth rates and metabolism activity.

MATERIAL AND METHODS

We analyzed two partial femora assigned to *Iberosuchus macrodon* Antunes 1975 from the Paleocene of La Boixedat (Spain). These specimens belong to the paleontological collections of the Institut Català de Paleontologia (ICP), labeled IPS4930 and IPS4932. In contrast to the condition in the Eusuchia, the femora of *Sebecus* and *Iberosuchus* are (a) straighter and (b) the medial edge of the greater trochanter is a prominent, sharp, longitudinal crest (Pol *et al.* 2012). Although the specimens in this study cannot be attributed unequivocally to *Iberosuchus* (whose holotype is a skull fragment), the morphological congruence of available specimens nevertheless justifies the assumption that the scarce, non-neosuchian Meoseucrocodylia specimens from the Paleogene of the Iberian Peninsula and southern France are at least closely related, indistinguishable forms (Ortega *et al.* 1996). We follow the phylogeny of Pol *et al.* (2012) in which Neosuchia and Notosuchia are sister taxa and *Iberosuchus* is a sebecosuchian nested in Notosuchia.

After photography, the bones were embedded under vacuum in a polyester resin, and two transverse slices, 3 mm in thick, were removed from the middle of the diaphysis (Fig. 1A, B) and the base of the proximal metaphysis (Fig. 1E, F) of each femur. According to standard ground section procedures (e.g. Lamm 2013), these slices were polished on one side, glued on glass slides and grounded to a thickness 100 µm ± 20. These thin sections were observed and photographed with a Nikon Eclipse E600POL microscope, under normal and cross-polarized light, with or without a lambda compensator.

Simple morphometric measurements were also performed on binary (black and white) images of the sections at mid-diaphysis (Fig. 1C, D) using the software Image J (Schneider *et al.* 2012). These measurements include: a) the compactness of each section, or GC (ratio, expressed in percent, of the area actually occupied by bone tissue to the total sectional area); b) compactness of the cortex proper, or CC (ratio, expressed in percent, of the actual area of the cortex occupied by bone tissue to the total cortical area, including bone plus cavities); c) the cortico-diaphyseal index, or CDi (mean thickness of bone cortex as a fraction of the mean diaphyseal radius).

RESULTS

Diaphyseal region of the femora

94 Both femoral diaphyses have a tubular morphology, with a free medullary cavity surrounded by a
95 compact cortex. However, specimen IPS 4930, though smaller than IPS 4932 (38 % less cross
96 sectional area) is clearly more compact (GC = 87.16% *vs* 77.52%) and has a thicker (CDi = 0.65 *vs*
97 0.54) and more compact (CC = 99.41% vs 79.06%) cortex. Perimedullary resorption is limited in this
98 specimen; as a consequence bone layers deposited in early ontogenetic stages are preserved.

99 Histologically, the bone forming the diaphyseal cortex has similar characteristics in the two
100 specimens. Most of its volume is predominantly composed of parallel-fibered tissue (Fig. 1A, B; Fig.
101 2A, B), displaying mass birefringence and collagen fiber bundles oriented circularly (i.e. parallel to the
102 outer contours of the bones). In IPS 4932, this tissue can locally turn to the lamellar type (Fig. 2B).
103 Frequent irregularities in the birefringence properties of the parallel-fibered bone suggest some degree
104 of local variation in fiber orientation. Cell lacunae in this tissue are oriented parallel to the collagen
105 fibers, and they display a small size, as compared to the lacunae occurring in primary or secondary
106 endosteal deposits forming e.g. osteons (Fig. 2C).

107 The vascularization of the primary cortex mainly consists of simple vascular canals oriented
108 longitudinally and, to a much lesser extent, obliquely. These canals are relatively few in the peripheral
109 (outer) part of the cortex; especially in IPS 4932 (Fig. 2A, B). Vascular density increases in deeper
110 cortical parts, a process much more pronounced in IPS 4930 (Fig. 1B; Fig. 2D) than in IPS 4932 (Fig.
111 1A). In both specimens, the cortical region bordering the medullary cavity has undergone Haversian
112 remodeling. This process was relatively diffuse in IPS 4932, where it created sparse secondary osteons
113 (Fig. 2C, E); it was more restricted but more intense in IPS 4930 where dense Haversian bone tissue
114 was spatially limited (Fig. 2F). Superficial resorption/reconstruction processes of variable intensity
115 also occurred around the medullary cavity, creating endosteal layers of secondary lamellar bone.

116 In both specimens the femoral cortex shows cyclical growth marks in the form of lines of arrested
117 growth (LAGs). The latter appear as thin dark lines parallel to the contour of the bones (Fig. 2G).
118 These lines are broadly, but unevenly, spaced in the depth of the cortex (280 µm in the average on Fig.
119 2G). In IPS 4932, the spacing of the LAGs suddenly becomes more regular and much narrower in the
120 most peripheral cortical layers, where the intervals between consecutive LAGs drop to 78 µm in the

121 average (Fig. 2G). Both femora also have bundles of short Sharpey's fibers (length 50 µm ± 10)
122 oriented radially and obliquely (Fig. 2H).

123 **Histology of the metaphyseal region**

124 The histological structure of primary periosteal cortices in the metaphyseal region of both
125 specimens (Fig. 1E, F) is basically similar to that prevailing in the diaphyseal region: most of the
126 cortical volume consists of parallel-fibered bone, the collagen fibers of which are oriented circularly
127 (Fig. 3A, B). However, three main differences exist. 1) Bone vascularization, mainly represented by
128 simple vascular canals and primary osteons oriented longitudinally, tends to be lower in the
129 metaphyses than in the diaphyses, especially in IPS 4930 (Fig. 3A, B). 2) Loose networks of
130 remodeled endosteal bone trabeculae (Fig. 1E, F; Fig. 3C) partly fill the medullary cavity (the
131 medullary cavity is free in the diaphysis). 3) In IPS 4932, the cortex is not only composed of
132 vascularized parallel-fibered tissue; but also contains a broad, central crescent-like meniscus formation
133 displaying different histological features (Fig. 1F; Fig. 3D). This formation is briefly described below.

134 This peculiar bone layer is located under the forth trochanter of the femur and consequently, it
135 occupies only a part of the sectional area (Fig. 1F). It is inserted in the middle of the cortex, between
136 two layers (under and above it) of ordinary parallel-fibered bone (Fig. 3D). Histologically, the thinnest
137 parts of this meniscus consist merely of some big longitudinal primary osteons (Fig. 3E). In its thicker
138 part, the meniscus displays two components: 1) Multiple oblong areas made of brightly birefringent
139 parallel-fibered tissue (blue in Fig. 3F, G) with a dominant, though variable, radial orientation
140 (including for cell lacunae) and vascular canals also displaying a gross radial orientation. 2) Small and
141 irregular monorefringent, or poorly birefringent areas, unevenly wedged between the birefringent
142 ones, and formed by woven bone (red in Fig. 3F, G). They contain big multipolar cell lacunae.

143 This basic structure can be interpreted in two distinct ways. The first interpretation is that it
144 represents former spongiosa, compacted by endosteal deposits. Crests, trochanters and other bone
145 excrescences related to muscle insertion are most often associated with spongy tissues within bone
146 cortices (e.g. Ricqlès 1976a). During growth, such spongiosae are frequently made compact by inter-
147 trabecular filling, a situation actually observed by one of us (VB) in sections of the fourth trochanter

of two alligatorids, *Alligator mississipppiensis* and *Diplocynodon ratelii*. The gross radial orientation of this compacted spongiosa in IPS 4932 reflects the strong traction stress exerted on the periosteum and the growing bone cortex by the muscle *caudofemoralis* (according to Wolf's law; cf. Currey 2002). An alternative interpretation of the meniscus structure is that it is made of a radiating fibro-lamellar bone complex, a tissue known to be characteristic of fast or very fast accretion. The monorefringent areas would represent the woven-fibered trabeculae initially deposited by the periosteum. The brightly birefringent areas would be primary osteons. The main difference between the bone forming the meniscus and typical fibro-lamellar complexes is that the highly ordered and conspicuous periosteal scaffoldings of woven-fibered trabeculae that characterize these complexes cannot be clearly identified in *Iberosuchus*. As a consequence, the limits and shape of the putative primary osteons cannot be traced precisely. For this reason, the tissue forming the thick part of the meniscus should be interpreted, with necessary caution, as an atypical form of radial fibro-lamellar bone tissue. Both interpretations, compacted spongiosa *vs* radiating fibro-lamellar complex, differ little from each other. In both cases, the differentiation of the fourth trochanter basically involves the sub-periosteal accretion of a spongiosa, and its subsequent compaction by inter-trabecular, centripetal deposits of endosteal lamellar or parallel-fibered tissue. Their main difference would reside in the dynamics of bone deposits: fast or very fast periosteal and endosteal deposits in the case of a radiating fibro-lamellar complex; much slower deposits in the case of a compacted spongiosa.

The basal part of the meniscus is in continuity (though histologically very distinct) with the subjacent parallel-fibered tissue. Conversely, the peripheral border of the meniscus is marked by a reversion line displaying a typical scalloped contour at high magnification (Fig. 3H). Above this line, towards bone periphery, the parallel-fibered tissue prevails again. The occurrence of this reversion line means that, during growth, the height of the basal part of the trochanter had to be reduced, through a resorption process, to become compatible with the diameter of the diaphysis into which the trochanter was sequentially relocated.

DISCUSSION

174 The most significant result of this study is that the femoral cortex of *Iberosuchus* is made of a
175 parallel-fibered tissue with variable vascular density and conspicuous lines of arrested growth. This
176 situation was observed in all bone sections, especially those sampled at mid-diaphysis, i.e. a sectional
177 plane classically considered as a general reference for histological studies of long bones; e.g. Lamm
178 2013). This result strongly suggests that *Iberosuchus* was not a fast growing, tachymetabolic animal,
179 but a slow growing crocodile with steep, cyclic decreases in growth rate. Several experimental studies
180 indeed show that, on the one hand, bone tissue with scattered longitudinal vascular canals results from
181 accretion speeds less than 5 µm/day (Castanet *et al*. 1996) and that, on the other hand, parallel-fibered
182 bone corresponds to accretion rates less than 1 µm/day (e.g. Buffrénil & Pascal 1984). The actual
183 apposition rate on the femoral cortex of *Iberosuchus* could have been between these values which are
184 anyway far below those prevailing for the woven-fibered tissue, especially when it contributes to the
185 constitution of fibro-lamellar complexes (laminar, plexiform, radiating bone tissues) typically
186 encountered in fast growing endotherms (Castanet *et al*. 1996, 2000; Margerie *et al*. 2002; see also
187 Cubo *et al*. 2012). In most modern crocodiles, the femoral cortex is made of a lamellar-zonal tissue
188 (Enlow & Brown 1957, Ricqlès 1976b, Lee 2004) displaying conspicuous yearly growth cycles. The
189 latter consist of zones made of woven-fibered tissue (that may change to the parallel-fibered type),
190 associated with annuli made of parallel-fibered or true lamellar bone (Buffrénil 1980a, b; Hutton
191 1986). These two components of an annual growth cycle are deposited sequentially and reflect a
192 progressive decrease in growth rate that may end, each year, in a total cessation of growth and the
193 formation of a LAG (Buffrénil 1980a). Since it integrates a woven-fibered component, the lamellar-
194 zonal tissue reflects faster deposition than the mere parallel-fibered type prevailing in *Iberosuchus*.
195 The occurrence of lines of arrested growth in this taxon, as well as the absence of annuli, clearly
196 shows that the maximum growth rate in *Iberosuchus* was comparable to the slowest rates of modern
197 crocodiles, and that growth stopped completely each year. As observable in the femur, the histological
198 features of *Iberosuchus* can be best compared to those of large predatory squamates such as the
199 varanids or the teids (e.g. Duarte-Varela & Cabrera 2000, Buffrénil & Hémery 2002, see also Cubo et
200 al. 2014). In both cases, bone cortices are made of parallel-fibered tissue (that may turn to the woven-
201 fibered type in the inner cortex) comprising longitudinal simple vascular canals or primary osteons,

202 and lines of arrested growth. Therefore, if the histological structure of long bones indeed reflects
203 growth rate, as initially proposed by Amprino (1947) and universally acknowledged today, then the
204 growth activity of *Iberosuchus* should be considered similar to that of extent large lizards. This
205 comparison is further substantiated by the spacing pattern of cyclical growth marks in IPS 4932.
206 Growth mark spacing indeed suggests that a sudden and steep decrease in growth activity occurred
207 about six years before this animal died. Its growth pattern was thus clearly asymptotic, a situation
208 commonly encountered in squamates in which epiphyseal and metaphyseal fusion limits growth
209 possibilities (Maisano 2008, Buffrénil *et al*. 2004). Conversely, this growth pattern is unusual in
210 crocodiles, though it was observed in some populations of *Alligator mississippiensis* (Woodward *et al*.
211 2011; see also Lee *et al*. 2013). IPS 4932 is larger than IPS 4930 and displays signs of a sudden
212 decrease in growth. These two characteristics indicate an older age for IPS 4932. Moreover, the
213 porosity of deep cortical layers in this specimen is a feature commonly encountered in mature
214 crocodilian females (Wink & Elsey 1986; Wink *et al*. 1987).

215 If the general relationship between the histological structure of primary bone cortices and their
216 appositional rate is now strongly evidenced by experimental data (e.g. Castanet et al. 1996), the
217 association between, on the one hand, bone tissue types and growth rate and, on the other hand, the
218 resting metabolic rate of an organism, seems to be less simple and less clearly deciphered. Montes et
219 al. (2007) found a direct relationship between periosteal bone growth rate and resting metabolic rate in
220 a sample of growing amniotes. In general, long bone cortices made of parallel-fibered tissue, be it
221 vascularized or not, are characteristically encountered in ecto-poikilothermic tetrapods (e.g. Enlow and
222 Brown 1956-1958, Ricqlès 1976). However, the few extant large squamates displaying vascular canals
223 (simple canals or primary osteons) within parallel-fibered bone, i.e. the largest Teidae (Duarte-Varela
224 & Cabrera 2000, Cubo et al. 2014) and the Varanidae more than 30 cm in snout-vent length (Buffrénil
225 et al. 2008), can experience transitory episodes of relatively high and constant metabolic rate during
226 either their reproductive cycle (Tattersall et al. 2016), or during times of intense foraging activity
227 (synthesis in Thompson 1999). Otherwise, these animals, including the largest ones, have a typical
228 ecto-poikilothermic physiology (Green et al. 1991, Christian & Conley 1994, Wikramanayake et al.

1999). The question is made more complex by the fact that the very same type of bone tissue (vascularized parallel-fibered bone) can be observed in long bone cortices in some large anurans, such as *Rana Catesbeiana*, *Rhinella marina,* or *Pipa pipa* (pers. obs. VB), known to have much lower metabolic rates than the squamates in general (White et al. 2006). Such observations suggest that the actual relationship between the details of bone structure and the metabolic rate of an organism result from a complex, multifactorial causality that needs to be fully deciphered. It nevertheless remains that bone cortices mainly composed of parallel-fibered tissue are very unlikely to belong to an endotherm-homeotherm animal. For this reason, the fundamental thermal regime of *Iberosuchus* should be considered to have been ectotherm and poikilotherm, as is also the case for the large extant squamates or lissamphibians mentioned above.

The particular case of *Iberosuchus* suggests that, in pseudosuchians, a terrestrial habitat is not necessarily associated with a high, sustained growth speed and the tachymetabolic regime consistent with it. Of course, this conclusion holds only for *Iberosuchus*. The Notosuchia (of which the Sebecosuchia are but one clade) represent a particularly rich and diversified lineage of terrestrial forms in which a number of bizarre and ecologically enigmatic taxa occur (e.g. Ortega *et al.* 2000). Future comparative studies should document whether this high morphological diversity also involved significant physiological discrepancies.

One element in our observations could challenge the conclusion presented above: the possible occurrence of radiating fibro-lamellar tissue in a limited area of the metaphyseal cortex of IPS 4932. This type of bone tissue is considered to result from the fastest accretion rate (Margerie *et al*. 2004) and is supposed to be an exclusive feature of fast-growing tachymetabolic tetrapods (Ricqlès 1974, 1976a). For several reasons, the occurrence of radiating fibro-lamellar tissue in the core of the metaphyseal cortex cannot be alleged to conclude that (1) episodes of fast growth occurred in the life of IPS 4932, and (2) that this taxon had the physiological competence for sustaining them at the level of the organism as a whole. As mentioned in the observations, the identification of this tissue is debatable, due to atypical histological characteristics. Nevertheless, even if the tissue forming the meniscus is really akin to fibro lamellar radiating bone, the complete lack of this tissue in diaphyeal

cortices (despite the excellent preservation of primary cortical tissues) would clearly indicate that its occurrence in the proximal metaphysis of IPS 4932 does not indicate a general trend towards fast growth in *Iberosuchus*, but a local, topographically restricted, process. This taxon might indeed have retained the potential capacity to develop fast periosteal accretion but, in the specimen studied here, this capacity would have been expressed in a strictly local context, in relation to the differentiation, growth and sequential relocation of the fourth trochanter during ontogeny.

With reference to the hypotheses listed in the introduction, our results suggest that the situation may be more complex than expected because some crocodyliforms might have preserved physiological potentialities that could have been expressed, or non-expressed, depending on morphological and/or ecological contexts. Future studies based on larger samples should settle more firmly this interesting question, and help assess if the capacity for fast growth, at least in limited skeletal regions and for a limited duration, is a frequent feature in the Notosuchia.

LITERATURE CITED

Amprino, R. 1947: La structure du tissu osseux envisagée comme expression de différences dans la vitesse de l'accroissement. *Archives de Biologie 58*, 315–330.

Antunes, M.T. 1975: Iberosuchus, crocodile Sébécosuchien nouveau, de l'Eocène ibérique au Nord de la Chaîne centrale, et l'origine du canyon de Nazaré. *Comunicaçoes dos Servicios Geologicos de Portugal 59*, 285-330.

Antunes, M.T. 1986: *Iberosuchus* et *Pristichampsus*, crocodiliens de l'Eocène : données complémentaires, discussion, distribution stratigraphique. *Ciències da Terra 8*, 111-122.

Buffrénil, V. de**.** 1980a: Données préliminaires sur la structure des marques de croissance squelettiques chez les crocodiliens actuels et fossiles*. Bulletin de la Société Zoologique de France 105*, 355-361.

Buffrénil, V. de. 1980b: Mise en évidence de l'incidence des conditions de milieu sur la croissance de *Crocodylus siamensis* (Schneider, 1801) et valeur des marques de croissance squelettiques pour l'évaluation de l'âge individuel. *Archives de Zoologie Expérimentale et Générale* 121, 63-76.

Buffrénil, V. de & Pascal, M. 1984: Croissance et morphogenèse postnatales de la mandibule du vison (*Mustela vison* Schreiber) : données sur la dynamique et l'interprétation fonctionnelle des dépôts osseux mandibulaires. *Canadian Journal of Zoology 62*, 2026-2037.

Buffrénil, V. de & Castanet, J. 2000 : Age estimation by skeletochronology in the Nile monitor (*Varanus niloticus*), a highly exploited species. *Journal of Herpetology 34*, 414-424.

Buffrénil, V. de & Hémery, G. 2002: Variation in longevity, growth, and morphology in exploited Nile monitors (*Varanus niloticus*) from sahelian Africa. *Journal of Herpetology 36*, 419-426.

Buffrénil, V. de, Ineich, I. & Böhme, W. 2004: Comparative data on epiphyseal development in the family Varanidae. *J. Herpetology 37*, 328-335.

Buffrénil, V. de, Clarac, F., Fau M., Martin, S., Martin B., Pellé, E. & Laurin, M. 2015: Differentiation and growth of bone ornamentation in vertebrates: a comparative histological study among the Crocodylomorpha. *Journal of morphology 276*, 425-445.

Castanet, J., Grandin, A., Abourachid, A., & Ricqlès, A. de. 1996: Expression de la dynamique de croissance dans la structure de l'os périostique chez *Anas platyrhynchos*. *Comptes-Rendus de. L'Académie des Sciences, Paris, Sciences de la Vie 319*, 301-308.

Castanet, J., Curry-Rogers, K., Cubo, J. & Boisard, J-J. 2000: Periosteal bone growth rates in extant ratites (ostrich and emu). Implications for assessing growth in dinosaurs. *Comptes-Rendus de. L'Académie des Sciences, Paris, Sciences de la Vie* 323, 543-550.

Christian, K.A. & Conley, K.E. 1994: Activity and resting metabolism of varanid lizards compared with "typical" lizards. *Australian Journal of Zoology 42*, 185-193.

Cubo, J., Le Roy, N., Martinez-Maza, C., Montes, L. 2012: Paleohistological estimation of bone growth rate in extinct archosaurs. *Paleobiology 38*, 335-349.

Cubo, J., Baudin, J., Legendre, L., Quilhac, A., Buffrénil, V. de 2014: Geometric and metabolic constraints on bone vascular supply in diapsids. *Biological Journal of the Linnean Society of London 112*, 668-677.

307 Duarte-Varela, C.F. & Cabrera, M.R. 2000: Testing skeletochronology in black tegu lizards
308 (*Tupinambis merianae*) of known ages. *Herpetologivcal Review 31*, 224-226.

309 Enlow, D.H. & Brown, S.O. 1957: A comparative histological study of fossil and recent bone tissues.
310 Part II. *Texas Journal of Science 9*, 186-214.

311 Farmer, C.G. and Sanders, K. 2010: Unidirectional Airflow in the Lungs of Alligators. *Science*
312 *327*, 338–340.

313 Green, B., King, D., Braysher, M., & Saim, A. 1991: Thermoregulation, water turnover and
314 energetics of free-ranging Komodo dragons, *Varanus komodoensis*. *Comparative Biochemistry and*
315 *Physiology 99A*, 97-101.

316 Hutton, J.M. 1986: Age determination of living Nile crocodiles from the cortical stratification of
317 bone. *Copeia* 1986(2), 332-341.

318 Lamm, E-T. 2013: Preparation and sectioning of specimens. *In* Padian, K., Lamm, E.-T. (eds): *Bone*
319 *Histology of Fossil Tetrapods*, 55–160. University of California Press, Berkeley.

320 Lee, A.H. 2004: Histological organization and its relationship to function in the femur of *Alligator*
321 *mississippiensis*. *Journal of Anatomy 204,* 197-207.

322 Legendre, L.J., Segalen, L. and Cubo, J. 2013: Evidence for high bone growth rate in *Euparkeria*
323 obtained using a new paleohistological inference model for the Humerus. *Journal of Vertebrate*
324 *Paleontology 33*, 1343–1350.

325 Legendre, L.J., Guénard, G., Botha-Brink, J. and Cubo, J. 2016: Paleohistological evidence for
326 ancestral high metabolic rate in archosaurs. *Systematic Biology 65,* 989-996.

327 Macleod, N., Rawson, P.F., Forey, P.L., Banner, F.T., BoudagherFadel, M.K., Bown, P.R.,
328 Burnett, J.A., Chambers, P., Culver, S., Evans, S.E., Jeffery, C., Kaminski, M.A., Lord, A.R., Milner,
329 A.C., Milner, A.R., Morris, N., Owen, E., Rosen, B.R., Smith, A.B., Taylor, P.D., Urquhart, E. and
330 Young, J.R. 1997: The Cretaceous-Tertiary biotic transition. *Journal of the Geological Society 154*,
331 265–292.

Maisano, J.A. 2002: Terminal fusion of skeletal elements as indicators of maturity in squamates. *Journal of Vertebrate Paleontology, 22*, 268-275.

Margerie, E. de, Cubo, J. & Castanet, J. 2002: Bone typology and growth rate: testing and quantifying « Amprino's rule » in the mallard (*Anas platyrhynchos*). *Comptes-Rendus de. L'Académie des Sciences, Paris, Sciences de la Vie* 325, 221-230.

Margerie, E. de, Robin, J-P., Verrier, D., Cubo, J. & Groscolas, R. 2004: Assessing the relationship between bone microstructure and growth rate: a fluorescent labelling study in the king penguin chick (*Aptenodytes patagonicus*). *Journal of Experimental Biology 207*, 869-879.

Montes, L., Le Roy, N., Perret, M., Buffrénil, V. de, Castanet, J. & Cubo, J. 2007: Relationship between bone growth rate, body mass and resting metabolic rate in growing aminotes: a phylogenetic approach. *Biological Journal of the Linnean Society 92*, 63-76.

Ortega, F., Buscalioni, A.D. and Gasparini, Z. 1996: Reinterpretation and new denomination of *Atacisaurus crassiproratus* (Middle Eocene; Issel, France) as cf *Iberosuchus* (Crocodylomorpha, Metasuchia). *Geobios 29*, 353–364.

Ortega, F., Gasparini, Z., Buscalioni, A.D. and Calvo, J.O. 2000: A new species of *Araripesuchus* (Crocodylomorpha, Mesoeucrocodylia) from the Lower Cretaceous of Patagonia (Argentina). *Journal of Vertebrate Paleontology 20*, 57–76.

Pol, D., Leardi, J.M., Lecuona, A. and Krause, M. 2012: Postcranial Anatomy of *Sebecus Icaeorhinus* (crocodyliformes, Sebecidae) from the Eocene of Patagonia. *Journal of Vertebrate Paleontology 32*, 328–354.

Ricqlès, A. de. 1974: Evolution of endothermy: histological evidence. *Evolutionary Theory 1*, 51-80.

Ricqlès, A. de. 1976a: Recherches paléohistologiques sur les os longs des tetrapods. VII. – Sur la classification, la signification fonctionnelle et l'histoire des tissus osseux des tetrapodes. *Annales de Paléontologie 62*, 71-126.

Ricqlès, A. de. 1976b: On bone histology of fossil and living reptiles, with comments on its functional and evolutionary significance. *In* Bellairs, A. d'A. & Cox, C.B. (eds) *Morphology and Biology of Reptiles*, 123-150. Linnean society Symposium Series n°3, London.

Ricqlès, A. de. 1978: Recherches paléohistologiques sur les os longs des tetrapods. VII. – Sur la classification, la signification fonctionnelle et l'histoire des tissus osseux des tétrapodes (troisième partie). *Annales de Paléontologie 64*, 85-111.

Ricqlès, Ad., Padian, K. & Horner, J.R. 2003: On the bone histology of some Triassic pseudosuchian archosaurs and related taxa. *Annales de Paléontologie 89, 67–101.*

Ricqlès, A. de, Padian, K., Knoll, F., Horner, J.R. 2008: On the origin of high growth rates in archosaurs and their ancient relatives: Complementary histological studies on Triassic archosauriforms and the problem of a "phylogenetic signal" in bone histology. *Annales de Paléontologie 94*, 57-76.

Riff, D. and Armin Kellner, A.W. 2011: Baurusuchid crocodyliforms as theropod mimics: clues from the skull and appendicular morphology of Stratiotosuchus maxhechti (Upper Cretaceous of Brazil). *Zoological Journal of the Linnean Society 163*, S37–S56.

Schneider, C.A. Rasband, W.S. and Eliceiri, K.W. 2012 : NIH Image to ImageJ: 25 years of image analysis. *Nature methods 9(7),* 671-675.

Seymour, R.S., Bennett-Stamper, C.L., Johnston, S.D., Carrier, D.R. and Grigg, G.C. 2004: Evidence for endothermic ancestors of crocodiles at the stem of archosaur evolution. *Physiological and Biochemical Zoology 77*, 1051–1067.

Summers, A.P. 2005: Evolution - Warm-hearted crocs. *Nature 434*, 833–834.

Tattersall, G.J., Leite, C.A.C., Sanders, C.E., Cadena, V. ,Andrade, D.V., Albe, A.S., Milson, W.K. 2016 : Seasonal reproductive endothermy in Tegu lizards. Scientific Advances 2016 ; e1500951.

Thompson, G. 1999 : Goanna metabolism : different to other lizards, and if so, what are the ecological consequences ? *In* Horn, H.-G. & Böhme, W. (eds.) Advances in monitor research II. – *Mertensiella 11*, 79-90.

382 Wink, C.S. & Elsey, R.M. 1986: Changes in femoral morphology during egg-laying in *Alligator*
383 *mississippiensis*. *Journal of Morphology 189,* 183-188.

384 Wink, C.S., Elsey; R.M. & Hill, E.M. 1987: Changes in femoral robusticity and porosity during the
385 reproductive cycle of the female Alligator (*Alligator mississippiensis*). *Journal of Morphology 193*:
386 317-321.

387 White, C.R., Phillips, N.F., Seymour, R.S. 2006 : The scaling and temperature dependence of vertebrate
388 metabolism. *Biology Letters 2*, 125-127.

389 Wikramanayake, E.D, Ridwan, W. & Marcellini, D. 1999 : The thermal ecology of free-ranging
390 Komodo dragons, *Varanus komodoensis*, on Komodo Island, Indonesia. *In* Horn, H.-G. & Böhme, W.
391 (eds.) Advances in monitor research II. – *Mertensiella 11*, 157-166.

392 Woodward, H.N., Horner, J.R. & Farlow, J.O. 2011: Osteohistological evidence for determinate
393 growth in the American alligator. *Journal of Herpetology 45*, 339-342.

394

395 **ACKNOWLEDGEMENTS**

396 We thank Francisco Ortega for his valuable help in performing the taxonomic assignment of
397 the samples analyzed to *Iberosuchus*. We would like to express our gratitude to an anonymous
398 reviewer for his/her helpful comments and to an associate editor for his/her stylistic suggestions. This
399 work was supported by the Spanish Ministry of Economy and Competitiveness: CGL2015-63777-P,
400 PI: MK, and 2014 SGR 1207, PI: MK, and CERCA Programme / Generalitat de Catalunya. We have
401 no conflict of interest to declare.

402

403 **FIGURE LEGENDS**

404 Figure 1: Gross aspect of the sections.

405 A: Global aspect of the the mid-diaphyseal section in IPS 4930. B: Global aspect of the the mid-
406 diaphyseal section in IPS 4932. C: Binary image of the mid-diaphyseal section in specimen IPS 4930.

D: Binary image of the mid-diaphyseal section in specimen IPS 4932. E: Global aspect of the the metaphyseal section in IPS 4930. F: Global aspect of the metaphyseal section in IPS 4932. Scale bar: 2 mm.

Figure 2: Bone histology in the femoral diaphysis in IPS 4930 and 49832.

A: Peripheral cortex of the femur in IPS 4930. The upper part is viewed in transmitted polarized light with lambda compensator; the lower part in ordinary transmitted light. B: Peripheral cortex of the femur in IPS 4932. Upper part: transmitted polarized light with lambda compensator; lower part: ordinary light. C: Size of osteocyte lacunae in periosteal and endosteal deposits (IPS 4932). The insert is a closer view at the wall of a secondary osteon as compared to the primary periosteal cortex. D: vascular density in the deep, peri-medullary cortex of IPS 4930. E: Secondary osteons scattered in the cortex of specimen IPS 4932. Polarized light. F: Localized area of dense Haversian tissue around the medullary cavity in IPS 4930. G: Lines of arrested growth, or LAG (arrows) in the cortex of IPS 4932. Note the tight spacing of the last LAGs. H: Sharpey's fibers in the cortex of IPS 4930 (arrows). All scale bars are equal to 0.5 mm but that of the close-up in C, which equals 0.1 mm.

Figure 3: Histological characteristics of the metaphyseal region.

A: Basic appearance of the femoral cortex in the metaphyseal region of IPS 4930. Upper part: transmitted polarized light with lambda compensator; lower half: ordinary transmitted light. B: Femoral cortex in the metaphyseal region of IPS 4932. Upper part: transmitted polarized light with lambda compensator; lower half: ordinary transmitted light. C: Remodeled endosteal trabeculae occupying the medullary cavity in the metaphysis of IPS 4930. Polarized light. D: Complex cortical structure observed locally in the metaphyseal of IPS 4932. The inner (left) and the outer (right) parts of the cortex are formed by parallel-fibered bone, the collagen fibers of which are oriented circularly (yellow). In between these layers the cortex is occupied by a tissue with a dominant radial structuration. E: Longitudinal primary osteons in the thin extremities of the crescent-like meniscus. Polarized light. F: Complex histological organization in the thick parts of the meniscus. Brightly birefringent (here in blue) and poorly birefringent (here in red) areas oriented radially are unevenly inter-mixed. Polarized light with lambda compensator. G: Continuity of the basal, parallel-fibered part

of the cortex (bottom part of the picture) with the tissue forming the meniscus. Polarized light with lambda compensator. H: Reversion line (RL) separating the meniscus and the peripheral layer of parallel-fibered bone tissue. The insert shows the typical scalloped contour of the reversion line. All scale bars are equal to 0.5 mm but that of the close-up in H, which equals 0.1 mm.

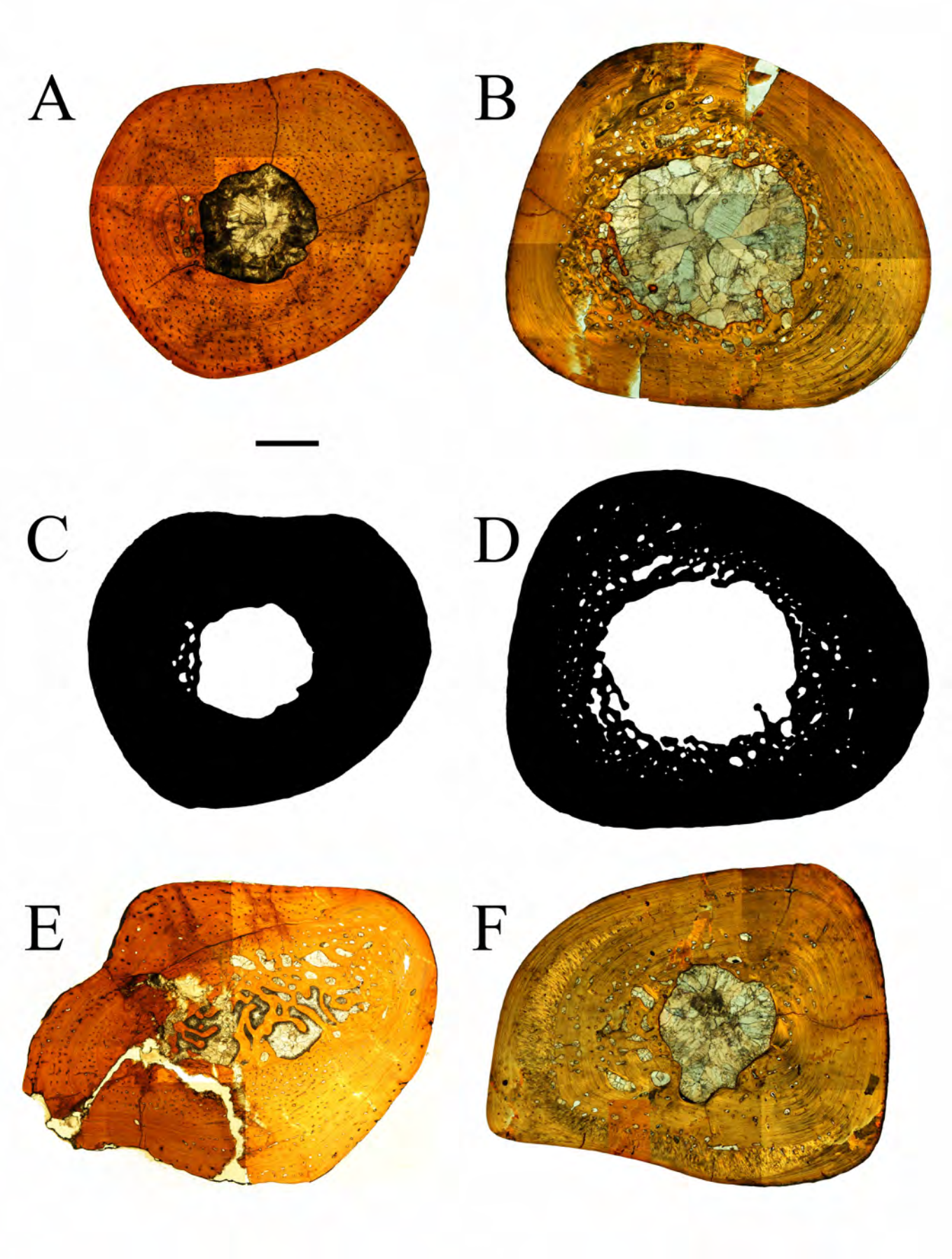
A
B
C
D
E
F

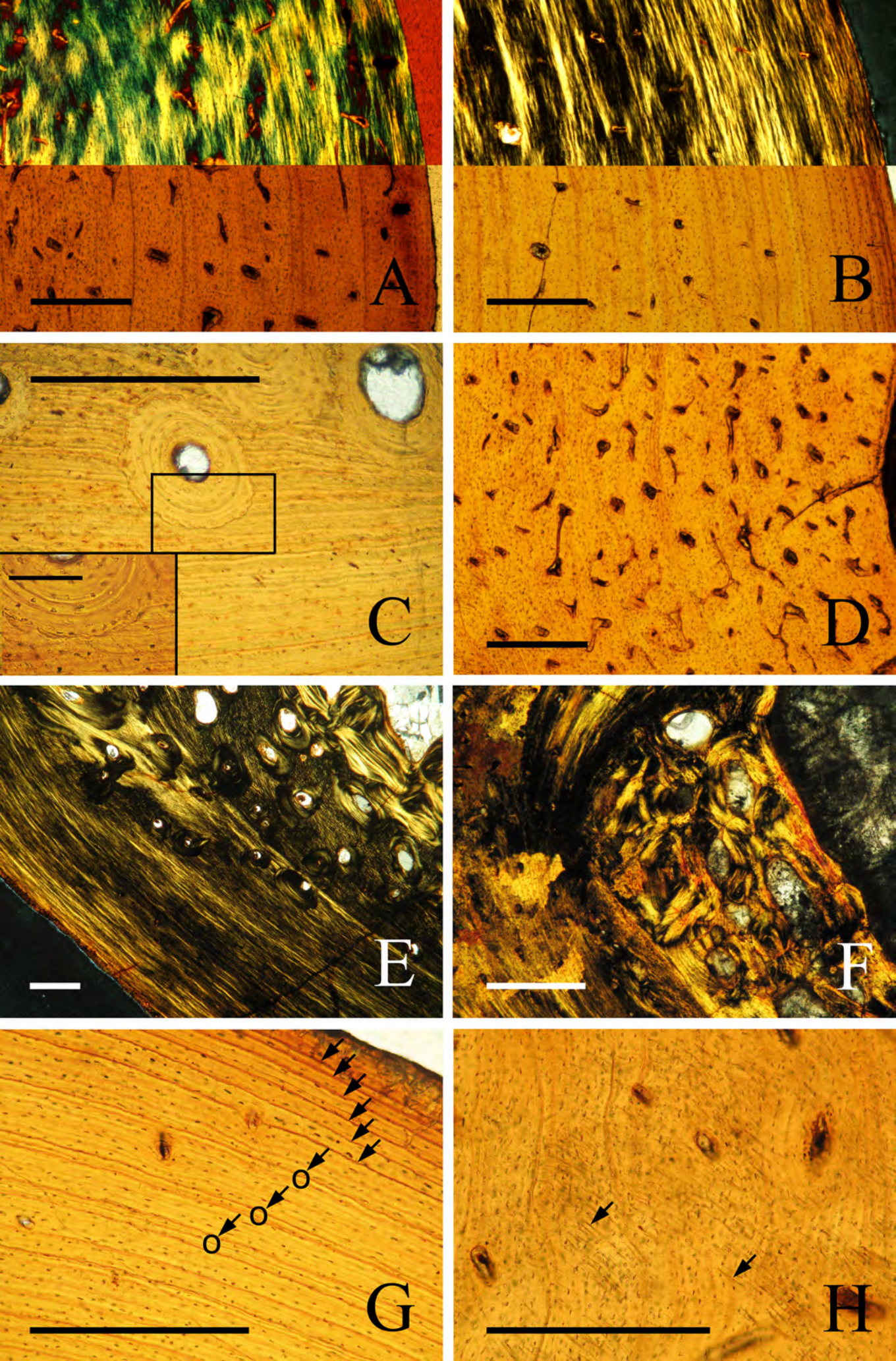
A
B
C
D
E
F
G
H

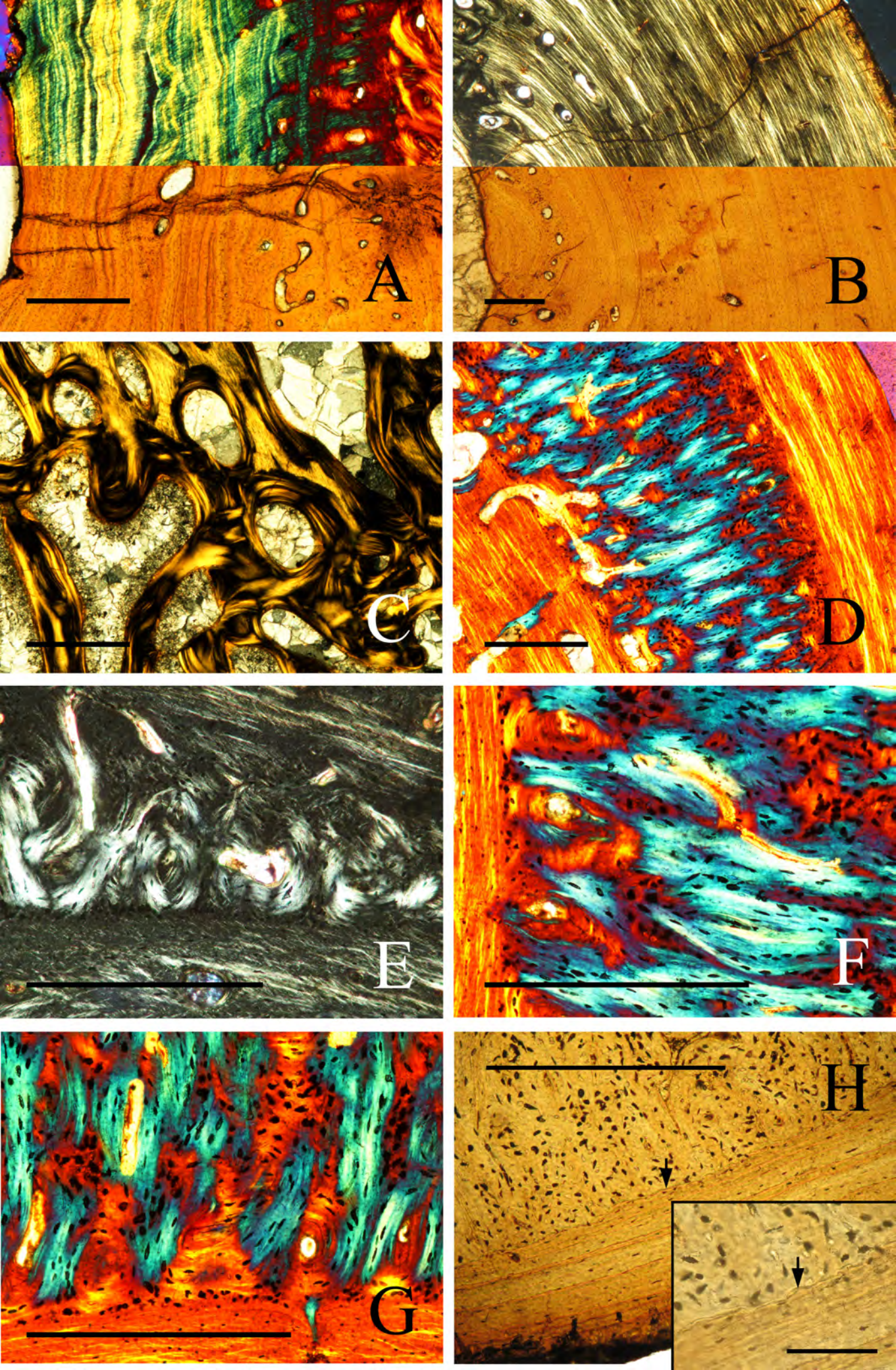
A
B
C
D
E
F
G
H